Model for Triplet−Triplet Energy Transfer in Natural Clusters of Peridinin Molecules Contained in *Dinoflagellate*'s Outer Antenna Proteins

Donatella Carbonera and Giovanni Giacometti*

Dipartimento di Chimica-Fisica, Università di Padova, Via Loredan 2, I-35131 Padova, Italy

Ulderico Segre

Dipartimento di Chimica, Università di Modena, Via Campi 183, 41100 Modena, Italy, and CSSMRE CNR, Via Loredan 2, I-35131 Padova, Italy

Alexander Angerhofer

Department of Chemistry, University of Florida, Gainesville, Florida

Ulrich Gross

3. Physikalisches Institut, Universität Stuttgart, Stuttgart, Germany

Received: December 4, 1998

Triplet−triplet energy transfer among peridinin molecules in peridinin−chlorophyll−protein (PCP) complexes from two different *dinoflagellate* species is quantitatively evaluated by the use of the optically detected magnetic resonance technique supplemented by triplet-state decay rate measurements. The two complexes are related by a dimer−monomer relationship in the sense that the four peridinins−one chlorophyll cluster of the *Heterocapsa pygmeae* PCP (H−PCP) is a copy of the two clusters contained in the larger protein *Amphidinium carterae* PCP (A−PCP), which are related by a local 2-fold symmetry axis. The system is conveniently discussed as a multistate Frenkel exciton system performing stochastic jumps from one exciton state to another. The rate of triplet−triplet energy exchange among peridinin molecules is obtained through the simulation of the spectral line shapes of optically detected magnetic resonance in zero field. Measurements were collected in a range of temperatures between 2 and 40 K and supplemented by the determination of the decay rate of the triplet to ground state in the same temperature range. The latter is of the order of 0.005 MHz and is relevant in determining the line shapes, especially at the lowest temperatures where the exchange rates are low. Exchange rates within the four-member peridinin cluster of H−PCP exactly match those within each of the two clusters of A−PCP and span a range from 0 to 20 MHz for the uphill rate and from 10 to 300 MHz for the downhill rate, corresponding to an energy difference of 41 cm^{-1}. The intercluster exchange rate in A−PCP goes from 0 to 12 MHz uphill and from 0.05 to 30 MHz downhill, with an energy difference of only 12.5 cm^{-1}. The kinetics conform to phonon-stimulated radiationless transition theory, and coupling parameters and reorganization energies are evaluated and discussed.

Introduction

Triplet−triplet energy-transfer rates are interesting from a theoretical point of view because of their relationship with electron-transfer rates.[1] Both processes are usually described by the well-known nonadiabatic phonon-assisted radiationless transition theory, which goes back to Kubo and Lax,[2,3] and now by the classical intervention of Marcus,[4] which has been further developed by Jortner[5] and many others.[6] The theory has been used successfully for the understanding of electron-transfer reactions in chemical systems and also of subtle details of primary events of charge separation in the photosynthetic reaction center.[7] For triplet−triplet transfer, a noteworthy research effort was started by the Argonne group[8] on synthetic systems made of intramolecular dyads of donor−acceptor molecules. From another point of view, triplet−triplet energy transfer was thoroughly studied in special solid-state collective systems where exciton and trap equilibrium and dynamics are measured by spectroscopic techniques, both optical and magnetic.[9−11]

In natural systems where one main function is that of transferring electronic excitation energy from molecule to molecule, as in pigment−protein complexes of the photosynthetic antennas and reaction centers, singlet exciton dynamics is of primary interest.[12] For triplet-state energy transfer, interesting situations have been investigated in antennas and reaction centers dealing with the photoprotective process of chlorophyll-to-carotenoid triplet transfer[13−19] and with the triplet exchange among the two components of the primary donor dimer.[20]

We have recently shown how magnetic resonance, optically detected at zero field (ODMR), is able to reveal triplet−triplet energy transfer within clusters of peridinin molecules contained in the peridinin−chlorophyll−protein (PCP) complexes which constitute the external antenna of *dinoflagellate* photosystems.[21]

* Corresponding author. E-mail: g.giacometti@chfi.unipd.it. Fax: +39-049-8275135.

10.1021/jp984641g CCC: $18.00
Published on Web 07/13/1999

In these systems, peridinin triplet states are formed by energy transfer from the chlorophyll *a* triplet state, which is formed under illumination. The structure and the mutual relationships of two PCP's obtained from the species *Heterocapsa pygmeae* (H−PCP) and *Amphidinium carterae* (A−PCP) are described in the preceding paper in connection with optical studies.[22] The chromophore disposition in A−PCP consists of two identical clusters made each of four peridinin molecules and one chlorophyll *a* molecule. In H−PCP, only one such cluster is present, which is supposed to be identical to the former as inferred from the large homologies of the corresponding polypeptides.

In this paper, we will expand the results obtained in ref 21 and construct a quantitative kinetic model of triplet−triplet energy transfer in the two PCP complexes. As suggested in ref 21, we will consider exactly the same exciton interactions within each cluster and further weaker interactions between the two clusters of A−PCP.

If the decay rates of the triplet states are of the order of the energy-transfer rates, they also affect the stationary state obtained under continuous illumination and, consequently, the ODMR line shapes. Triplet-state decay rates are determined by transient absorption experiments, and the appropriate parameters for the modified Bloch equations which simulate the experimental line shapes are determined for each temperature. The results are then discussed in terms of the nonadiabatic radiationless transition theory.

The dynamic results obtained in this paper acquire increased interest in view of the optical data discussed in ref 22 based on the recent determination of the molecular structure of A−PCP provided by an X-ray crystallographic investigation.[23]

Materials and Methods

The ODMR data are obtained by fluorescence detection as described in ref 21. The results given there are supplemented further by data collected in the present work and are fully consistent with the previous ones. The temperature range investigated is limited to the 2−40 K range because, as shown elsewhere,[24] a different process affecting the line shapes and zero-field splittings sets in above 40 K, which is not described with the analysis presented here.

Triplet State Decay Rate Measurements. Transient absorption experiments were performed with the instrumental setup described in ref 25 with a time resolution of approximately 20 ns. Briefly, an excimer-pumped dye laser was used to excite the sample using DCM (4-dicyanomethylene-2-methyl-6-[(*p*-dimethylamino)styryl]-4*H*-pyran) as the laser dye and an excitation wavelength around 668 nm to pump the chlorophyll *a* Q_y band.

A tungsten lamp was used to provide the cw probing light, perpendicular to the laser excitation. Appropriate filter combinations were used to limit the probing light to a narrow bandwidth of approximately ±10 nm around the peridinin triplet−triplet absorption at 565 nm.

The transients were recorded with a Le Croy 9450 transient digitizer from the output of an avalanche photodiode which was used to detect the probe beam.

Modified Bloch Equation Analysis. In the simulation of the triplet ODMR spectra, we started from the model proposed by Burland and Zewail[26] in the analysis of coherent spectroscopy in electronically excited states. According to this model, two triplet levels ($|a\rangle$ and $|b\rangle$) connected by the microwave field are picked up from the excited states manifold, and the density matrix method is adopted to describe the dynamics of the two-level system (TLS). The remaining levels are considered only as sources and sinks for the TLS populations.

The energy spacing ($h\nu_0$) between the two levels is given by a static Hamiltonian (H_0), and the TLS is driven by an oscillating field with frequency $\omega = 2\pi\nu$ and strength $\omega_1 = \gamma_e B_1$, inducing radiative transitions between the levels. Nonradiative transitions $W_{a\rightarrow b} \equiv W_a$ and $W_b = W_a \exp(-h\nu_0/k_B T)$, as well as the dephasing relaxation rate (T_2^{-1}), are included into the equation of motion of the density matrix of an isolated TLS.

An additional decay rate term is added to the equation of motion of the density matrix elements:

$$\frac{d\rho_{ij}}{dt} = -\frac{1}{2}(k_i + k_j)\rho_{ij} \qquad (i, j = a, b) \tag{1}$$

This term represents phenomenologically the interaction with the remaining states of the real system. In a similar way, the feeding rates also can be included in the equation of motion of ρ. We do not devise a detailed model to describe the birth of the population of the TLS, but instead we assume simply that it occurs incoherently so that only the diagonal elements of the density matrix are affected. Therefore, the Liouville equation for the density matrix elements in the rotating frame turns out to be

$$\frac{dr_1}{dt} = -(\bar{k} + \bar{W} + T_2^{-1})r_1 - 2\pi\Delta\nu r_2 \tag{2a}$$

$$\frac{dr_2}{dt} = 2\pi\Delta\nu r_1 - (\bar{k} + \bar{W} + T_2^{-1})r_2 - \omega_1(\rho_{aa} - \rho_{bb}) \tag{2b}$$

$$\frac{d\rho_{aa}}{dt} = \frac{\omega_1}{2}r_2 - (k_a + W_a)\rho_{aa} + W_b\rho_{bb} + F_a \tag{2c}$$

$$\frac{d\rho_{bb}}{dt} = -\frac{\omega_1}{2}r_2 - (k_b + W_b)\rho_{bb} + W_a\rho_{aa} + F_b \tag{2d}$$

where $r_1 = \rho_{ab} + \rho_{ba}$, $r_2 = i(\rho_{ab} - \rho_{ba})$, $\bar{k} = (k_a + k_b)/2$, $\bar{W} = (W_a + W_b)/2$, and $\Delta\nu = \nu_0 - \nu$. The differential equation system (1) can be rewritten in matrix form as

$$\dot{\rho} = \mathbf{L}\rho + \mathbf{F} \tag{3}$$

where $\boldsymbol{\rho}$ is a four-dimensional vector with components (r_1, r_2, ρ_{aa}, ρ_{bb}) and the vector $\mathbf{F} = (0, 0, F_a, F_b)$ is formed by the feeding rates. The absorption line shape is obtained from the steady-state solution for the density matrix by putting $\dot{\boldsymbol{\rho}} = 0$ into eq 3 and is given by $r_2(\nu)$, i.e., the imaginary part of the off-diagonal element ρ_{ab}.[26]

The above model can be readily extended to include exchange between two or more different excited triplet states, whose density matrixes are indicated as ρ_p and with energies E_p. The modification of eq 3 is straightforward in the case that the zero-field-splitting tensors of the triplets share the same principal axes. We indicated with K_{pq} the jump rate from site p to site q. Then, the equation of motion can be written in the spirit of the McConnell modification[27] as

$$\dot{\boldsymbol{\rho}}_p = \mathbf{L}_p\boldsymbol{\rho}_p + \sum_q(\boldsymbol{\rho}_q K_{qp} - \boldsymbol{\rho}_p K_{pq}) + \mathbf{F}_p \tag{4}$$

The line shape in the general case is just the sum of the r_2 elements for the various sites computed under steady-state conditions.

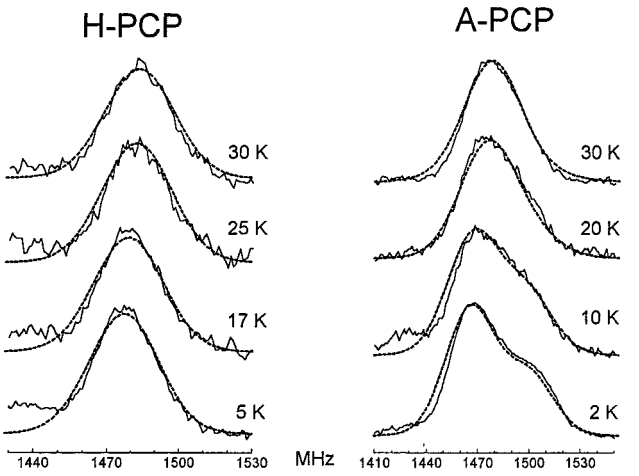

Figure 1. Line-shape fits of the D + E transition in *Heterocapsa pygmaea* PCP and in *Amphidinium carterae* PCP. Simulation parameters are given in Table 1.

The assumption of parallel principal axes for the interacting triplet states is justified on the grounds that the transitions originating from the pair of levels used for each system are so well separated (frequency 800−1000 MHz), from the other two possible transitions, when compared with the kinetic rates involved (1−100 MHz), that the third level of each system is seen as totally fixed by the radiation field.

Results

First of all, we report the results of peridinin triplet-state decay measurements done on H−PCP and A−PCP at various temperatures between 2 and 300 K. The decay rates are equal within the experimental errors, for both complexes, and temperature independent up to 200 K. In this range, they can be fitted with two exponentials. These two rates reflect the anisotropy of the triplet sublevel dynamics, showing two fast unresolved rates ($\tau = 13\ \mu$s) and a slower one ($\tau = 58\ \mu$s) as usually found in carotenoid systems.[28] The ODMR measurements are analyzed only in the case of the D + E transitions. These transitions are about 6 times more intense than the D − E transitions and, compared to the 2E transitions, show two well-resolved components at very low temperatures in the case of A−PCP complex. For these reasons, the D + E transition is the most suitable for the kinetic analysis. According to transient EPR experiments performed on carotenoid triplet states,[29] the D + E transition involves two-level decaying, the upper one with a fast rate and the lower one with a slower rate; these two rates correspond to the two exponentials contained in the measured triplet decay.

Peridinin triplet-state D + E transitions are reported for the two complexes at a number of temperatures in Figure 1. In the H−PCP case, the line shape appears always as a single transition and shifts somewhat toward high frequency with the rise in temperature. The small signal appearing on the low-frequency side has been found to arise from a different triplet species and will be discussed elsewhere.[24] In the A−PCP case, on the contrary, splitting into two lines at low temperatures is evident and merging into one line occurs at higher temperatures.

The quantitative analysis of the data is now based on the kinetic scheme of Figure 2 where the four lowest states of the eight peridinin molecule double cluster of A−PCP are shown and are correlated with the two lowest states of the four peridinin molecule cluster of H−PCP. It is assumed that the parameters regulating the dynamics of the H−PCP cluster are the same as

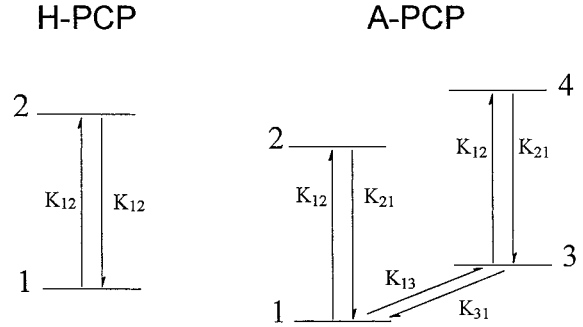

Figure 2. Kinetic scheme of triplet−triplet energy transfer among peridinin exciton states in *Heterocapsa pygmaea* and *Amphidinium carterae* PCP proteins.

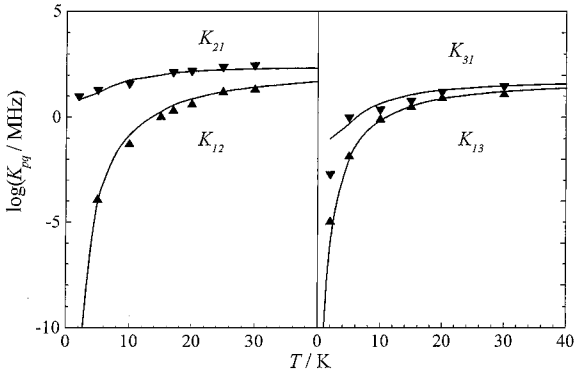

Figure 3. Behavior of energy-transfer rates K_{12}, K_{21} and K_{13}, K_{31} with temperature. Theoretical plots are from eq 10. Parameters values (cm^{-1}): $h\nu = 10$; $\Delta E_{12} = 41$; $E_{r12} = 155$; $V_{12} = 0.76$; $\Delta E_{13} = 13$; $E_{r13} = 136$; $V_{13} = 0.35$.

those of each of the two A−PCP clusters. Upper states are considered not reachable at the temperatures of the experiments, as there is no evidence of their presence in the kinetics.

The model is characterized by a number of parameters that are determined by a global analysis on the two complexes throughout the temperature range of the experiments.

The parameters can be divided into four categories.

The first category includes the parameters taken from experimental measurements. These are the decay rates k_a and k_b, taken to be independent of the temperature and equal to $0.017 \times 10^6\ s^{-1}$ (0.003 MHz) and $0.077 \times 10^6\ s^{-1}$ (0.012 MHz), respectively (see above). The ODMR transition frequencies of the two low-energy triplet states in A−PCP (1 and 3 in the scheme of Figure 3) are taken as the experimental values observed at the lowest temperature available (1467 and 1500 MHz, respectively), while for those of H−PCP (1 and 2) we take the values already obtained in ref 21 by the approximation of the fast exchange regime (1478 and 1538 MHz, respectively). In the case of A−PCP, we also need the values for the frequencies of the low population states 3 and 4 of the scheme arising from the intercluster coupling. These are taken in such a way that intracluster splitting is equal to that of H−PCP and intercluster splitting of the upper doublet is equal to that of the lower one ($\nu_0^{(2)} - \nu_0^{(1)}$ and $\nu_0^{(4)} - \nu_0^{(3)}$ are equal and the frequencies $\nu_0^{(1)}$ and $\nu_0^{(3)}$ are symmetrically situated with respect to the H−PCP frequency of 1478 MHz measured at low temperatures).

The second group of parameters consists of the inhomogeneous and homogeneous line widths. While the latter do not influence the results as long as care is taken to use a number of sampling points that is sufficiently dense (a nominal value of 1 MHz was used in the calculations), the inhomogeneous width

TABLE 1: Parameters and K_{ij} Values (MHz) at Different Temperatures As Obtained from Global Fits of D + E Transition Line Shapes[a]

T, K	K_{12}	K_{21}	K_{13}	K_{31}
2	0	10 ± 2	$<1 \times 10^{-5}$	0.002 ± 0.0015
5	$<1 \times 10^{-4}$	20 ± 2	0.020 ± 0.002	1.0 ± 0.1
10	0.050 ± 0.006	40 ± 3	1.3 ± 0.1	2.4 ± 0.3
15			3.0 ± 0.2	6.0 ± 0.5
17	2.0 ± 0.2	140 ± 11		
20	4.0 ± 0.6	160 ± 15	8 ± 1	16 ± 2
25	15 ± 2	250 ± 30		
30	20 ± 3	300 ± 40	12 ± 2	30 ± 3

[a] Temperature independent parameters: $F_a = 4$; $F_b = 2$; $k_a = 0.003$; $k_b = 0.012$; $W_a = W_b = 0$; $1/T_2 = 1$. H-PCP: $\nu_0^{(1)} = 1478$; $\nu_0^{(2)} = 1538$. A-PCP: $\nu_0^{(1)} = 1467.5$; $\nu_0^{(2)} = 1527.5$; $\nu_0^{(3)} = 1501$; $\nu_0^{(4)} = 1561$; inhom. width = 14.

has to be determined by the global analysis. Full width at half-maximum (fwhm) values of 13−14 MHz (Gaussian line shape) were found to be adequate.

The third category of parameters is the rates K_{pq} which are determined by the global analysis. Cross rates K_{14}, K_{24}, K_{23}, and K_{41}, K_{42}, K_{32} have been neglected since we can safely assume that the intracluster rates (K_{12}, K_{34} and K_{21}, K_{43}) are much faster. The only processes connecting the two clusters are those corresponding to K_{13} and K_{31}.

There is a fourth category of parameters, contained in eqs 2a−d, namely, the relaxation rates (W_p) and pumping rates from the reservoir (F_p), but they should affect only the signal intensities (not the shapes). We then neglected all relaxations and used constant values for the population rates of the upper and lower levels of each triplet state. All the lines are then normalized to the experimental intensity.

The complete results obtained by the global fitting are reported in Table 1, and examples of the fits are shown in Figure 1.

It has to be noted again that exactly the same rate parameters and frequency splittings are used for H−PCP and for each of the two clusters of A−PCP; hence, the only new parameters used for the simulation of the line shapes in the case of the latter are the rates K_{13} and K_{31}.

The line-shape asymmetry found at low temperatures for A−PCP (see Figure 1) is produced in a situation where the two lower lying exchanging triplet states are equal in their populating and decay rates. The intensity difference occurs because the two states are decaying fast with respect to the exchange rates and a slight energy difference between the two states produces the asymmetry at low temperatures (k_BT less than the energy difference). In other words, at low temperatures, exchange is frozen out compared to triplet decay.

The kinetic parameters have been reported in Table 1 with an indication of error ranges. They were estimated in the course of the global analysis by determining the limits of the rate parameters between which no sensible varation of the fitted line shapes was observed. The low-temperature values ($T < 5$ K) are the only ones affected by the values measured for ka and kb; hence, their error margins are larger. The K_{13} value at 2 K is immeasurably low.

Discussion

The triplet states labeled 1−4 in Figure 2 can be thought as exciton states of the type

$$|T_p\rangle = \sum_q C_{pq}|t_q\rangle \qquad (5)$$

where $|t_q\rangle$ represent the localized peridinin triplet states and C_{pq} are coefficients determined by the exciton interaction matrix. It is well-known that states of this sort may have different energies and also different zero-field splittings even when the unperturbed zero-order states are degenerate.[30] Of course, differences due to the different environments provided by the polypeptide cage can be also considered. The energy differences then arise both from the electron interaction matrix elements among the $|t_q\rangle$ states and from the "site" effects. Zero-field-splitting differences, causing different ODMR frequencies for each state, arise also from possible site effects but especially from spin−orbit coupling, according to the general expression

$$\Delta\omega = (\xi/\Delta_{S-T})^2(\delta_S - \delta_T) \qquad (6)$$

where ξ is a spin−orbit coupling matrix element, Δ_{S-T} is the singlet−triplet energy separation, and δ_S and δ_T are the exciton splittings in the singlet and triplet states, respectively.

From the phenomenological point of view, it does not matter which is the origin of the energy and frequency differences among the peridinin triplet states, and it is not easy to assign the effects to one or to the other cause. Excitonic interaction is certainly present and might cause or enhance the frequency differences. The order of magnitude of the spin−orbit coupling necessary to account for the estimated frequency differences, as deduced from eq 6, is in fact reasonable, as already discussed in ref 21. The system is then conveniently described as a multistate Frenkel exciton[31,32] system performing stochastic jumps from one state to another. In the Frenkel limit, owing to phonon scattering, there is a partial localization of the electronic excitation, but still a coherent propagation is possible as a wave packet, provided that the explicit linear combination of eq 5 remains unchanged for times exceeding the time associated with the electronic intermolecular interaction. In molecular crystals such as tetrachlorobenzene, where electronic intermolecular interaction is topologically unidimensional and the coherence analysis is feasible,[11] for typical electronic exchange energies of about 0.35 cm^{-1}, it has been found that the number of molecules in an exciton linear chain at cryogenic temperatures is of the order of 5000. Since, as we shall see below, the electronic coupling energies appear to be of the same order of magnitude, it is not at all unreasonable to speak of coherent excitons within our small peridinin multimers.

We now discuss the estimated values of the rates as obtained from the ODMR line shapes and their temperature behavior by using the theory of phonon-assisted radiationless transitions. For triplet-state excitation energy transfer (TEET), the theory follows exactly the well-known lines of electron transfer (ET) and the rate is given[4] by a Fermi golden rule expression

$$K = (4\pi^2/h)|V|^2\mathrm{FC} \qquad (7)$$

where V is the electronic interaction and FC is the temperature-dependent Franck−Condon factor.

The electronic interaction for TEET is given[1] by a matrix element that, in the case of localized triplet states, corresponds to an electron interaction which is proportional to the product of two overlap integrals (the donor−acceptor LUMO−LUMO and HOMO−HOMO overlap integrals, respectively):

$$V \propto S^{DA}{}_{LL} S^{DA}{}_{HH} \qquad (8)$$

To compare with an electron-transfer process, the corresponding V value would be proportional only to the overlap between the

LUMO orbitals (S^{DA}_{LL}). This justifies the much smaller triplet-transfer couplings with respect to electron-transfer ones.

The Franck−Condon factor (FC) was given in many different ways, and nice compact limiting expressions were derived in the low-temperature and high-temperature limits.[6] For exoergic processes, the low-temperature limit corresponds to the quantum mechanical tunneling rate across the energy barrier of the process. The energy barrier can be traced to the Marcus[4] expression:

$$E_{act} = (\Delta E - E_r)^2/4E_r \quad (9)$$

where E_r is the medium reorganization energy and ΔE the reaction energy gap.

Since we are dealing with processes where energy differences are comparable to the k_BT values in the temperature range of the experiments, it is necessary to use a rate expression that is valid over the complete temperature range. One such expression is given by Jortner,[33] who considers the coupling with a single phonon with energy $h\nu$ sufficiently low not to overcome the lowest energy gap of the model (Einstein-type "soft" model):

$$K_{pq} = (4\pi^2/h)(|V_{pq}|^2/h\nu)\exp[-s(2\zeta+1)]I_r\{2s[\zeta(\zeta+1)]^{1/2}\}[(\zeta+1)/\zeta]^{r/2} \quad (10)$$

where $s = E_s/h\nu$ is the reduced electron−phonon coupling, $r = |\Delta E_{pq}|/h\nu$ is the reduced energy gap, $I_r\{x\}$ is a modified Bessel function of order r, and $\zeta = [\exp(h\nu/k_BT) - 1]^{-1}$ is the Bose factor. First we simulate the temperature dependence for the *Heterocapsa* processes for which we have already a good value for the energy difference estimated from the frequency shifts produced by the temperature changes. Figure 3 shows the fitting obtained for the two rates K_{12} and K_{21}, and the fitting parameters are collected in Table 1. As one can see, the temperature behavior is in good agreement with the theory. The value of the parameter ΔE_{12} is quite close to that obtained previously[21] from a simple analysis of the temperature-dependent shifts of the spectral lines. The result is not very sensitive to the choice of $h\nu$, which has been taken to be equal to 10 cm^{-1}, of the order of the smallest energies involved. The value of E_s is quite low as expected for triplet−triplet adiabatic transfer (no net charge shift involved) as compared with the usual electron-transfer values in normally activated reactions.

The value of V_{12} has an order of magnitude (0.8 cm^{-1}) that is in agreement with estimated values for other known cases. It is clear, however, that this value is not adequate to explain the much larger energy differences among the excitonic states (40 cm^{-1}). The interaction matrix elements for the excitonic mixing are to be calculated on peridinin triplet wave functions ($|t_q\rangle$ states of eq 5), while the analogous matrix elements determining the jump rate are to be calculated among the exciton wave functions ($|T_p\rangle$ states of eq 5), and we then recognize that energy splittings may well be different than what one would predict from the knowledge of the V factors in the rate expression. More importantly, the influence of the locally different protein environment affecting the zero-order state energies of the peridinin components of the exciton must be considered.

Figure 3 shows that also the intercluster rates K_{13} and K_{31} are well described by the phonon-assisted radiationless rate theory and the determined parameters are in line with the structural notions we have on the complexes. The energy difference of the lowest states of the two clusters is indeed very small ($\Delta E_{13} = 12.5$ cm^{-1}). Here again it is not easy to say how much of the difference is due to small site effects. The E_s value again is of the same order as that found for the intracluster processes. The electronic coupling that we found ($V_{13} = 0.35$ cm^{-1}) is less than one-half that of the intracluster interaction.

Conclusions

In this paper, triplet−triplet energy transfer among peridinin molecules in PCP complexes from two different *dinoflagellate* species is quantitatively evaluated by the use of the optically detected magnetic resonance technique supplemented by triplet-state decay rate measurements. This is the first example of a natural system where such measurements could be achieved in a convenient range of temperatures such as to be in a position to test at least a simple version of nonadiabatic phonon-assisted radiationless transition theory, the one often employed in electron-transfer processes.

The two complexes are related by the fact that one is twice the other, and the larger presents a quasi 2-fold local symmetry between the two halves. They are described by triplet−triplet transfer models which are totally in agreement with the view that the energetics within each of the two halves of the double complex is the same and is identical to that of the smaller complex. The structure of the latter is not known from X-ray crystallography, but the polypeptide sequence suggests a very similar structure for the five pigments cluster.[22]

In the large complex, the two halves are also subjected to intercluster triplet−triplet energy exchange, and the energetics is fully coherent with the smaller interactions involved.

A comment is in order here about the optical properties of the A−PCP complex (absorption and CD spectra) which have been calculated from the knowledge of the X-ray structure[22] and an evaluation of the long-range electronic interactions between peridinin and chlorophyll molecules. Relevant interactions are found both within each cluster and between the two clusters, and moreover, the intercluster interactions are essential to describe some important features of the CD spectrum. In view of the fact that optical and CD spectra of H−PCP are practically identical to those of A−PCP, the conclusion was drawn that H−PCP also behaves in solution as a dimeric protein molecule stabilized by noncovalent interactions with an overall structure very similar to that of the larger covalent "dimer".

The fact that triplet exchange among the two clusters is negligible in H−PCP as found from the ODMR experiments is not in contradiction with the above findings. Triplet migration is mediated by short-range electronic interactions, and the detailed structure of the protein cage is probably determining the difference between the covalent and the noncovalent complexes. It would be of interest to investigate if an analysis of the possible different electron paths in the two cases according to Onuchic and Beratan theories[34] is going to give us an account of the different V_{ij} values that have been determined in our experiments, namely, that the ratio between intercluster and intracluster interactions is about one-half in the covalent A−PCP dimer, while it should be significantly less in the noncovalent H−PCP dimer. The search should be feasible given the accurate structure of the A−PCP complex now available.

Acknowledgment. This investigation was supported in part by Italian MURST under program BIOSTRUTT and by EC Contract No. ERB FMRX-CT98-0214 (DG 12-MZLS); both agencies are gratefully acknowledged.

References and Notes

(1) Closs, G. L.; Johnson, M. D.; Miller, J. R.; Piotrowiak, P. *J. Am. Chem. Soc.* **1989**, *111*, 3751−3753.

(2) Kubo, R. *Phys. Rev.* **1952**, *86*, 929−937.
(3) Lax, M. *J. Chem. Phys.* **1952**, *20*, 1752−1760.
(4) Marcus, R. A. *Angew. Chem., Int. Ed.* **1993**, *32*, 1111−1121.
(5) Jortner, J. *J. Chem. Phys.* **1976**, *64*, 4860−4867.
(6) Ulstrup, J. *Charge-Transfer Processes in Condensed Media*; Springer: Berlin, 1979.
(7) Bixon, M.; Jortner, J.; Michel-Beyerle, M. E. In *Reaction Centers of Photosynthetic Bacteria*; Michel-Beyerle, M. E., Ed.; Springer: Berlin, 1990; pp 389−400.
(8) Sigman, M. E.; Closs, G. L. *J. Phys. Chem.* **1991**, *95*, 5012−5017.
(9) Fajer, M. D.; Harris, C. B. *Phys. Rev.* **1974**, *B9*, 748.
(10) Harris, C. B.; Fajer, M. D. *Phys. Rev.* **1974**, *B10*, 1784−1800.
(11) Dlott, D. D.; Fajer, M. D. *Chem. Phys. Lett.* **1976**, *41*, 305−310.
(12) van Grondelle, R.; Dekker: J. P.; Gillbro, T.; Sundstrom, V. *Biochim. Biophys. Acta* **1994**, *1187*, 1−65.
(13) Groot, M. L.; Peterman, E. J.; van Stokkum, I. H.; Dekker, J. P.; van Grondelle, R. *Biophys. J.* **1995**, *68*, 281−290.
(14) Peterman, E. J.; Dukker, F. M.; van Grondelle, R.; van Amerongen H. *Biophys. J.* **1995**, *69*, 2680−2688.
(15) Young, A. J.; Frank, H. A. *J. Photochem. Photobiol. B, Biol.* **1996**, *36*, 3−15.
(16) Frank, H. A.; Chynwat, V.; Posteraro, A.; Hartwich, G.; Simonin, I.; Scheer, H. *Photochem. Photobiol.* **1996**, *64*, 823−831.
(17) Farhoosh, R.; Chynwat, V.; Gebhard, R.; Lugtenburg, J.; Frank, H. A. *Photochem. Photobiol.* **1997**, *66*, 97−104.
(18) Peterman, E. J.; Gradinaru, C. C.; Calkoen, F.; Borst, J. C.; van Grondelle, R.; van Amerongen, H. *Biochemistry* **1997**, *36*, 12208−12215.
(19) Laible, P. D.; Chynwat, V.; Thurnauer, M. C.; Schiffer, M.; Hanson, D. K.; Frank, H. A. *Biophys. J.* **1998**, *74*, 2623−2637.
(20) Sieckmann, I.; Brettel, K.; Bock, C.; Vanderest, A.; Stehlik, D. *Biochemistry* **1993**, *32*, 4842−4847.
(21) Carbonera, D.; Giacometti, G.; Segre, U. *J. Chem. Soc, Faraday Trans.* **1996**, *92*, 989−993.
(22) Carbonera, D.; Giacometti, G.; Segre, U.; Hofmann, E.; Hiller, R. G. *J. Phys. Chem.* **1999**, preceding paper in this issue.
(23) Hofmann, E.; Wrench, P. M.; Sharples, F. P.; Hiller, R. G.; Welte, W.; Diederichs, K. *Science* **1996**, *272*, 1788−1791.
(24) Gross, U.; Angerhofer, A.; Giacometti, G.; Wolf, H. C. Manuscript in preparation.
(25) Angerhofer, A.; Bornhauser, F.; Gall, A.; Cogdell, R. J. *Chem. Phys.* **1995**, *194*, 259−274.
(26) Burland, D. M.; Zewail, A. H. *Adv. Chem. Phys.* **1979**, *40*, 369−484.
(27) McConnell, H. *J. Chem. Phys.* **1958**, *28*, 430−431.
(28) Frank, H. A.; Bolt, J. D.; Costa, S. M. d. B.; Sauer, K. *J. Am. Chem. Soc.* **1980**, *102*, 4893−4898.
(29) Carbonera, D.; Di Valentin, M.; Corvaja, C.; Agostini, G.; Giacometti, G.; Liddell, P.; Kuciauskas, D.; Moore, A.; Moore, T. A.; Gust, D. *J. Am. Chem. Soc.* **1998**, *120*, 4398−4405.
(30) Zewail, A. H.; Harris, C. B. *Phys. Rev. B* **1975**, *11*, 935.
(31) Frenkel, J. *Phys. Rev.* **1931**, *37*, 17.
(32) Frenkel, J. *Phys. Rev.* **1931**, *37*, 1276.
(33) Jortner, J. *J. Am. Chem. Soc.* **1980**, *102*, 6676.
(34) Onuchic, J. N.; Beratan, D. N.; Winkler, J. R.; Gray, H. B. *Annu. Rev. Biophys. Biomol. Struct.* **1992**, *21*, 349−377.